Chapter 2

Ultrasonic Machining: A Total Mechanical Machining Technology Using Loose Abrasive Particles

Jingsi Wang

Additional information is available at the end of the chapter

http://dx.doi.org/10.5772/intechopen.75170

Abstract

Although manufacturing technologies are well developed for materials like metals and their alloys, considerable problems still exist in the fabrication of hard and brittle materials including ceramics and glass. Their superior physical and mechanical properties lead to long machining cycle and high production cost. Ultrasonic machining (USM) using loose abrasive particles suspended in a liquid slurry for material removal is considered an effective method for manufacturing these materials. This work gives a brief overview of USM first and then mainly addresses the development of a simulation model of this process using a mesh-free numerical technique, the smoothed particle hydrodynamics (SPH). The crack formation on the work surface impacted by two abrasive particles is studied for understanding the material removal and the interaction of abrasive particles in USM. Experiments are also conducted to verify the simulation results. The SPH model is proven useful for studying USM and is capable of predicting the machining performance.

Keywords: ultrasonic machining, smoothed particle hydrodynamics (SPH), hard and brittle materials, material removal mechanism, hole drilling

1. Introduction

Hard and brittle materials, such as glass, ceramics, and quartz crystal, are getting more and more attention in the recent years due to their superior properties like high hardness, high strength, chemical stability, and low density. High-performance products made of these materials play an important role in various industrial fields including semiconductor, optical components, aerospace, and automotive industries [1, 2]. However, considerable problems such as long machining cycle and high production cost still exist in the fabrication of hard and brittle materials. Particular difficulties are the production of micro−/nanostructures with

high machining efficiency, high aspect ratios, and good surfaces possessing no residual stress and microcracks. Hence, there is a crucial need for developing precision and efficient micro-machining techniques for these materials.

Nontraditional machining techniques such as electric discharge machining and laser beam machining have been proposed to machine hard and brittle materials. However, even these processes have prominent limitations that the machined surfaces are always subjected to heat-induced damages like recast layer and thermal stress. Ultrasonic machining (USM) is another alternative method for manufacturing both conductive and nonconductive hard and brittle materials. It is known as a total mechanical process without suffering from heat or chemical effects, so USM would not thermally damage the machining objects or appear to cause significant levels of residual stress and chemical alterations.

However, not much research has been conducted to clarify the mechanism of USM up to date, and the knowledge for the process is far from sufficient to provide a complete understanding and instructive rules for practical use. Therefore, no further developments of micro-USM happened in recent years. In this work, a brief overview of USM is given first in Section 2. Then, a mesh-free numerical technique, the smoothed particle hydrodynamics (SPH), is introduced to simulate the USM process in Section 3, and its verification experiments are presented after that. The crack formation on the work surface impacted by two abrasive particles was studied in the simulation to reveal the material removal and the interaction of abrasive particles in USM. Finally, problems to be solved in order to put USM into an effective industrial micro-machining method are given. Further work should be conducted to clarify the nature of USM process for improving the machining performance.

2. Overview of ultrasonic machining (USM)

2.1. Principle of USM

Figure 1 shows a schematic of the basic elements of a USM apparatus used nowadays. High-frequency electrical energy can be converted into mechanical vibrations with resonant frequency via the transducer. The excited vibration is subsequently transmitted through an energy-focusing horn to amplify the vibration amplitude and finally delivered to the tool tip. Thus, the tool which locates directly above the workpiece can vibrate along its longitudinal axis with a desired high amplitude. A slurry comprising hard abrasive particles (generally using silicon carbide, boron carbide, and alumina) in water or oil is provided constantly into the machining area. During the fabrication of hard and brittle materials, a large number of tiny fractures occur on the work surface and lead to the material removal.

2.2. Features and potentialities of USM

Markov [3] classified workpiece materials into three categories in consideration of the USM suitability: the materials belonging to the first group, such as glass, mica, and quartz, are quite brittle and easy for USM process. The materials are removed by the initiation and propagation

http://dx.doi.org/10.5772/intechopen.75170

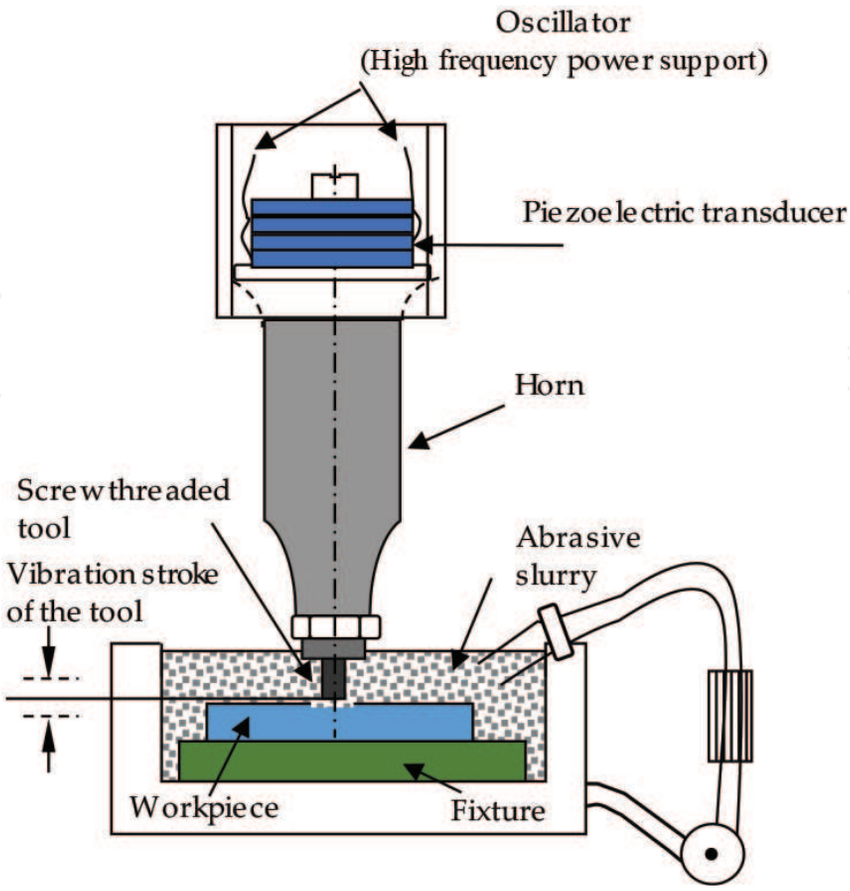

Figure 1. Schematic of basic elements in USM.

of tiny cracks of the workpiece in this situation. The second group includes the materials that exhibit some plastic deformation before fracture like titanium alloys, carburized, and nitrided steels. USM can machine these materials although with some difficulty. The last group consists of the ductile materials, such as soft steel and copper, and they are unsuitable in principle for USM. Note that a recent research reported that the ductile substrate materials are not really removed but are displaced, which also have been observed for some fine polishing operations [4]. The classification of the materials and fields of application for USM are given in **Table 1**.

USM has shown potentialities in many manufacturing uses; the most commonly ones are the fabricating structures of any shapes on hard and brittle materials. Hole drilling always stands as the most popular machining process for product manufacturing, and USM in particular shows a high potentiality in fabricating diverse holes either with large/small diameters or high aspect ratios. Masuzawa's group firstly proposed micro-USM as an effective micromachining process for hard and brittle materials. Holes with diameters as small as 5 μm and aspect ratios larger than 5 were successfully fabricated on quartz glass and silicon by micro-USM in one of their studies [6]. At the other extreme, tools with diameters as large as 85 mm were successfully employed for drilling holes with a high-capacity (2.5 kW) ultrasonic machine [7]. Besides, USM is playing an irreplaceable role in fabricating holes with a high

Group of material	Predominant type of deformation	Type of failure	Field of application of USM
I. Glass, mica, quartz, ceramic, diamond, germanium, silicon, ferrite, alsifer	Elastic	Brittle	Manufacturing parts of semiconducting materials Making industrial diamonds Fabricating special ceramics Manufacturing parts of glass quartz or minerals in the optical and jewelry industries Machining ferrite, alsifer, and other materials
II. Alloys tempered to high hardness carburized and nitrided steels, titanium alloys	Elastic–plastic	Brittle after work hardening by plastic deformation	Making and repairing hard alloy dies, press tools, and purchases Shaping or sharpening hard alloy tools
III. Lead, copper, soft steel	Plastic	No failure (or ductile failure)	Unsuitable for ultrasonic machining

Table 1. Classification of materials and fields of application for USM [3, 5].

aspect ratio. Micro-holes under 100 μm in diameter and aspect ratios of 10 on quartz glass were achieved by electrorheological fluid-assisted USM [8].

There also has been a heavy industrial demand for the fabrication of 3D microstructures on various hard and brittle materials. Two ways are used to achieve microstructures on hard and brittle materials via USM. One is by directly duplicating the tool shape on workpiece. In this way, complex 3D structures or multiple holes can be generated with a single pass of the machining tool. However, some problems including different machining rates over the whole working area and differential tool wear rate should be solved when using tools of complex form for keeping the product shape [9, 10]. Moreover, it is troublesome to fabricate micro-tools of complex shapes. The other one is to employ a simple "pencil" tool and contour the complex structures via a computerized numerical control (CNC) program. By using this method, machining any complex microstructures on hard and brittle materials accurately is possible. Sun et al. [11] have developed a 3D micro center-pin bearing air turbine using this method successfully, and the test results show that the turbine has a great reliability.

2.3. Involved material removal mechanism

The material removal mechanisms in basic USM were investigated quite intensively. Three well-recognized major removal actions were summarized by the previous researchers and include [5, 9, 12] (i) mechanical abrasion due to direct hammering of larger abrasive particles on the workpiece surface, (ii) microchipping resulted from the impact of free-moving abrasive particles, and (iii) cavitation erosion from the abrasive slurry. These mechanisms are schematically shown in **Figure 2**.

http://dx.doi.org/10.5772/intechopen.75170

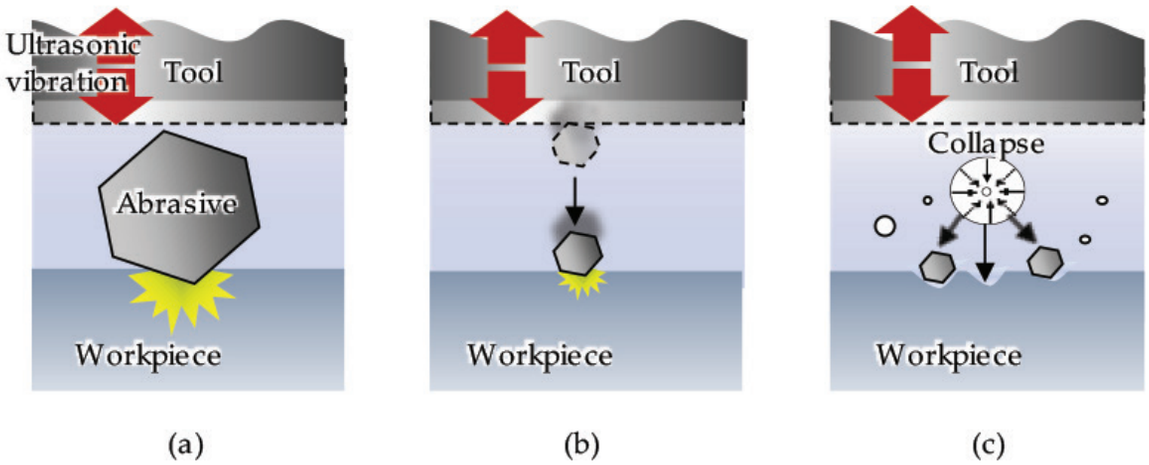

Figure 2. Schematic diagram of material removal mechanisms in USM: (a) hammering action, (b) impact action, and (c) cavitation erosion.

However, as it is difficult to observe the USM phenomena directly, a total understanding of the material removal is still not possible. Only qualitative evaluations according to experimental results were reported [13–15], except that an analysis model was established recently [16] based on the former study [17]. In other studies, the researchers concentrated on revealing the material removal mechanism [5, 18] by assuming the hammering of an abrasive particle in USM as an indentation process. However, the direct indentation process does not involve the actions including the tool vibration and abrasive fracture in USM; a more effective way for investigating and understanding the nature of material removal in USM is necessary.

The present author's group firstly proposed to study the influences of the hammering action and the impact action on material removal in USM process using a mesh-free numerical simulation method, smoothed particle hydrodynamics (SPH) [19]. The results are shown in **Figures 3** and **4**, respectively. One cycle of the tool vibration was simulated, and the fluid effect was not considered. Fractures occurred in both the abrasive and the workpiece after the hammering action as shown in **Figure 3(d)**. However, in the case of impact action, the accelerated abrasive due to the tool impact did not generate fractures and rebounded as depicted in **Figure 4(d)**, which means that the impact action is not effective for material removal on the raw work surface. The obtained results support the common view that hammering action plays a primary role in material removal of USM process [5].

2.4. Main process parameters

A large number of input parameters exist in USM process which would influence the machining performance. A cause and effect diagram to show the potential factors affecting USM is depicted in **Figure 5**. Influences of major process parameters on the material removal rate, machining precision, surface quality, and tool wear have been widely experimentally investigated.

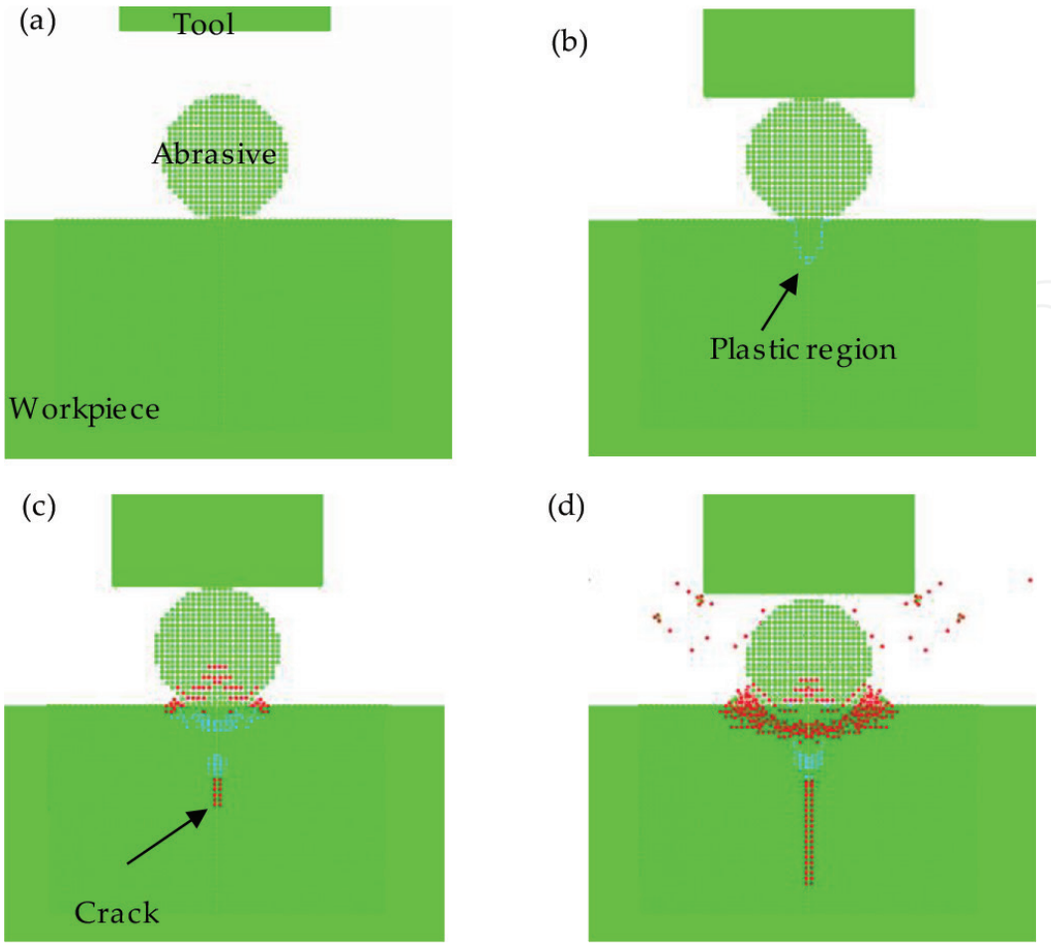

Figure 3. Simulation results of direct hammering action on the work surface: (a) before calculation, (b) after tool impact (0.1 μs calculation), (c) 1 μs calculation, and (d) after unloading.

Lee and Chan [18] investigated the influence of vibration amplitude, static load, and the particle size on the machining rate and surface roughness. They suggested that the material removal rate (MRR) would be increased, while the machined surface would be roughened with any increase in these parameters. Yu et al. [20] stated that the machining speed decreased with an increase in the static load beyond a certain level and the abrasive size was a dominant factor influencing the surface roughness in USM. Guzzo et al. [21] demonstrated an increase in material removal rate with larger abrasive particles due to the increase in the stress induced by the impact of these particles against the work surface. Komaraiah and Reddy [5] discussed the effects of mechanical properties of the workpiece on material removal rate and found that the hardness and fracture toughness of the workpiece material played an important role in ultrasonic machining. There was a reduction in material removal rate with the increase of the hardness and fracture toughness of the workpiece material. In another study of Komaraiah and Reddy [22], experiments were carried out to clarify the effect of tool materials on the material removal rate, tool wear, and surface quality. While a difficult-to-machine material can be machined effectively, the tool in USM was

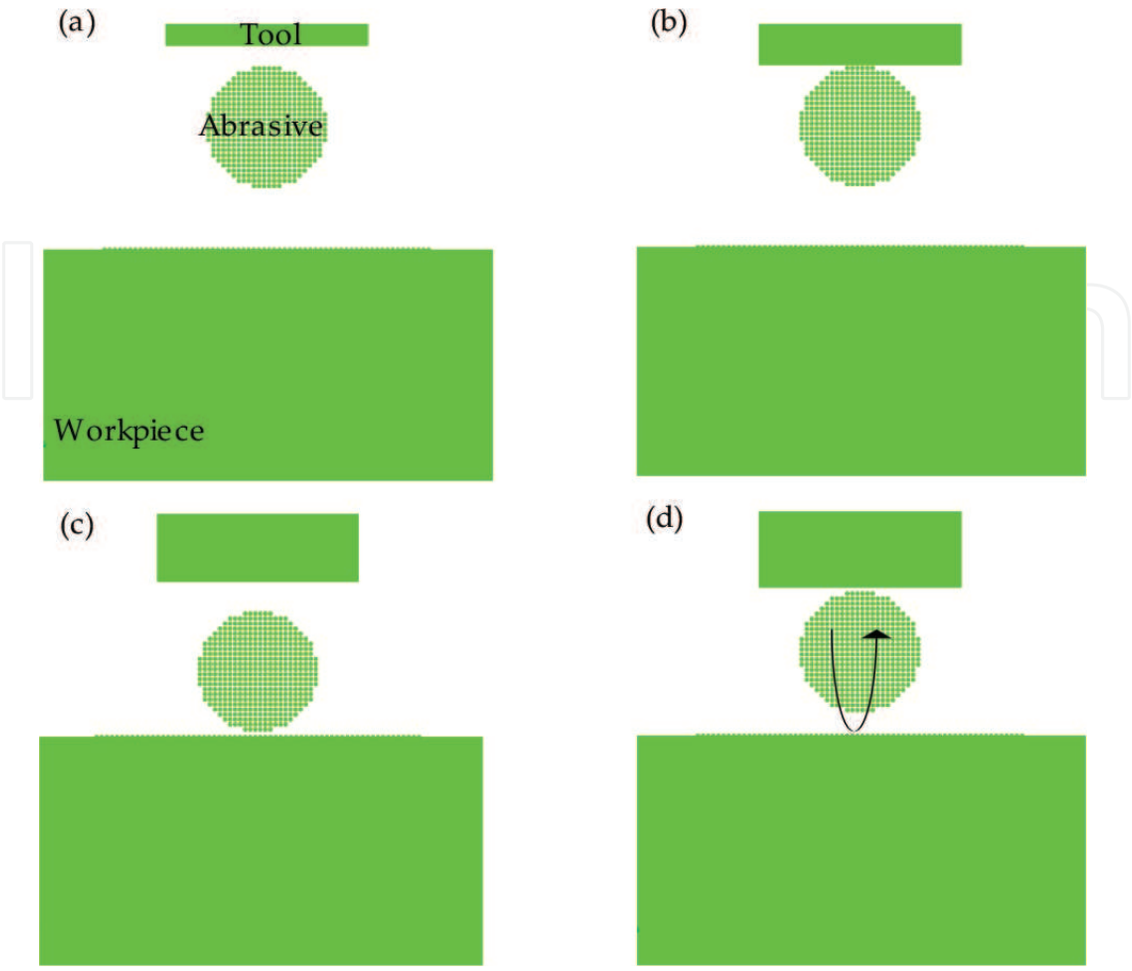

Figure 4. Simulation results of impact action: (a) before calculation, (b) after the tool impact on the abrasive particle, (c) after the particle impact on the work surface, and (d) rebound of the abrasive particle.

also worn. It was found that larger material removal rate, diametral tool wear resistance, and lower surface roughness can be obtained when using harder tool material. They also stated that both the hardness and the impact strength of the tool material would influence the longitudinal tool wear. Hocheng et al. [23] considered that large vibration amplitude increased the kinetic energy of abrasive particles, which wore the tool tip seriously, while a large static load depressed the free vibration of the abrasive particles and slowed down the tool wear.

Although many factors affect the machining performance of USM, it is believed that an optimum machining condition can be found to meet specific machining requirements. Further studies on the material removal mechanism in USM are extremely significant for understanding the influences of various process parameters on machining performance, which can provide a guidance in choosing suitable machining conditions and improve the machining performance.

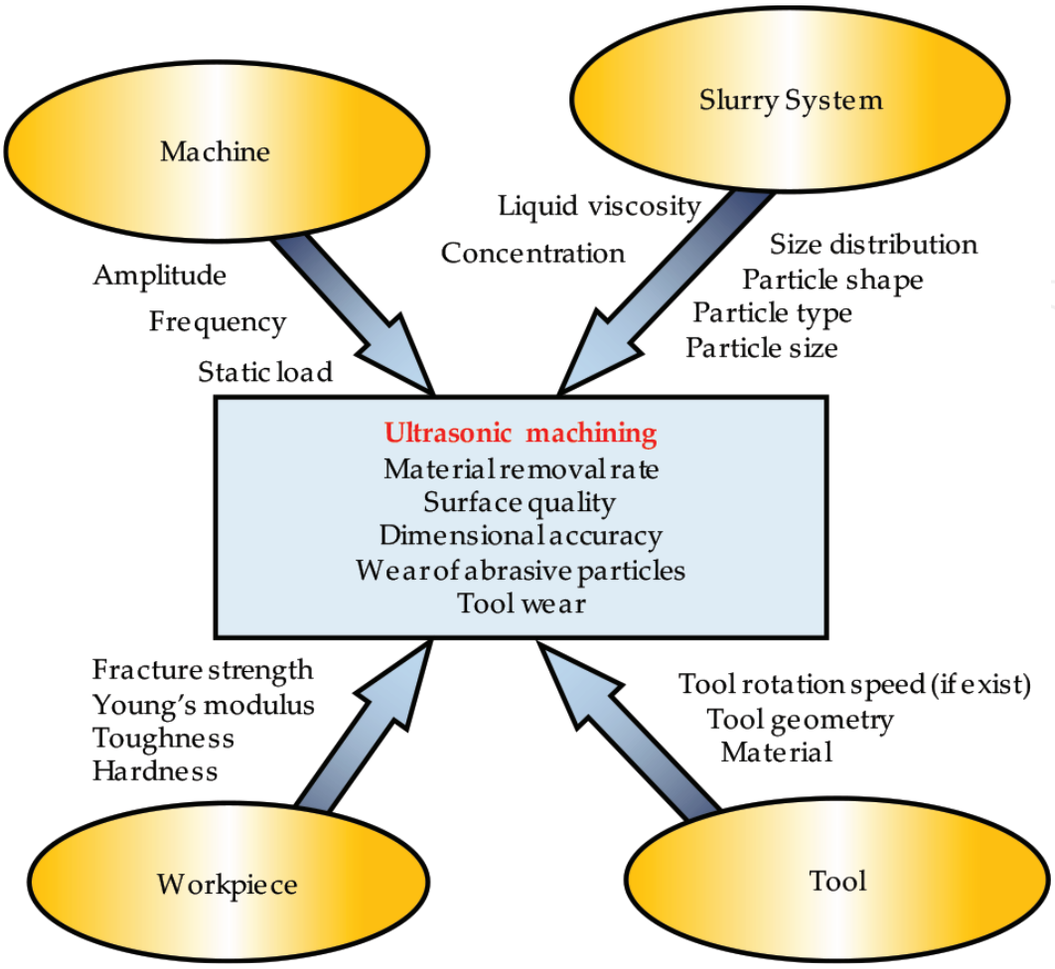

Figure 5. A cause and effect diagram for machining parameters in USM.

3. SPH simulation and experimental verification

3.1. Simulation method and results

3.1.1. Smoothed particle hydrodynamics (SPH)

SPH is a mesh-free numerical technique first introduced to solve astrophysics problems. In SPH, the system is represented by a set of particles that carry material properties and interact with each other according to the governing conservation equation. Problems involved in large deformation, which may cause errors due to mesh distortion and tangle with the grid-based method, can be effectively solved by the SPH. Thus, it is capable to simulate a USM process, in which material fracture occurs under repeated impacts of abrasive particles.

3.1.2. Material modeling

Glass, silicon carbide (SiC), and SS304 referred to stainless steel (AISI:304) were used for workpiece, abrasive, and tool material, respectively. Glass and SiC, which are hard and brittle, have

high compressive strength but low tensile strength; the Mie-Grüneisen polynomial equation of state was employed. On the other hand, the strength and damage behavior of these materials were modeled with Johnson-Holmquist material model [24, 25], in which fracturing occurs when the hydro tensile limit is reached. For SS304 material, the Shock equation of state was used, and the strength is formed by Steinberg-Guinan model. The constants related to the equations of the material models and material properties, for glass [26], SiC [27], and SS304 [28], are obtained from existing test data and summarized as shown in **Table 2**.

3.1.3. Modeling conditions and assumptions

In USM, a large number of abrasive particles act on the workpiece simultaneously by repeated impacts of the tool, and the hammering action dominates the main material removal. Therefore, the simulation model was built with two abrasive particles based on the direct hammering action to figure out influences of the interaction between adjacent abrasive particles on the process. **Figure 6** shows a snapshot of the model. The dimensions for each part is as defined in the figure. One half of the geometry was established with symmetric boundary conditions, and spherical abrasive particles were considered. The abrasive particle and the partial workpiece areas around the hammering site, where heavy deformation can occur, were built with SPH solver. The ultrasonically vibrated tool and the remaining parts of the workpiece were modeled by using the Lagrange finite element mesh. It is because that the SPH algorithm takes more time to find neighboring particles, which is usually more expensive in computation time. Materials in small deformation to be constructed with the grid-based Lagrange solver are helpful to reduce the calculation amount.

Figure 7 shows the moving conditions of the tool tip. The solid curve is the ideal condition given in the experiments: the tool tip vibrates sinusoidally with a frequency of 61 kHz and the total amplitude of 4 μm. Contrastingly, the dashed curve is the simplified condition for the calculation: the

	Float glass	**SiC**	**SS304**
Equation of state	Polynomial		Shock
Density (g/cm^3)	2.53	3.215	7.9
Bulk modulus (GPa)	45.4	220	None
Grüneisen coefficient (Γ)	None		1.93
Strength	Johnson-Holmquist		Steinberg-Guinan
Shear modulus (GPa)	30.4	193.5	77 (G_0)
Hugoniot elastic limit (GPa)	5.95	11.7	None
Yield stress (MPa)	None	None	340 (Y_0)
Failure	Johnson-Holmquist		None
Hydro tensile limit (MPa)	150	750	None

Table 2. Material models and relevant parameters.

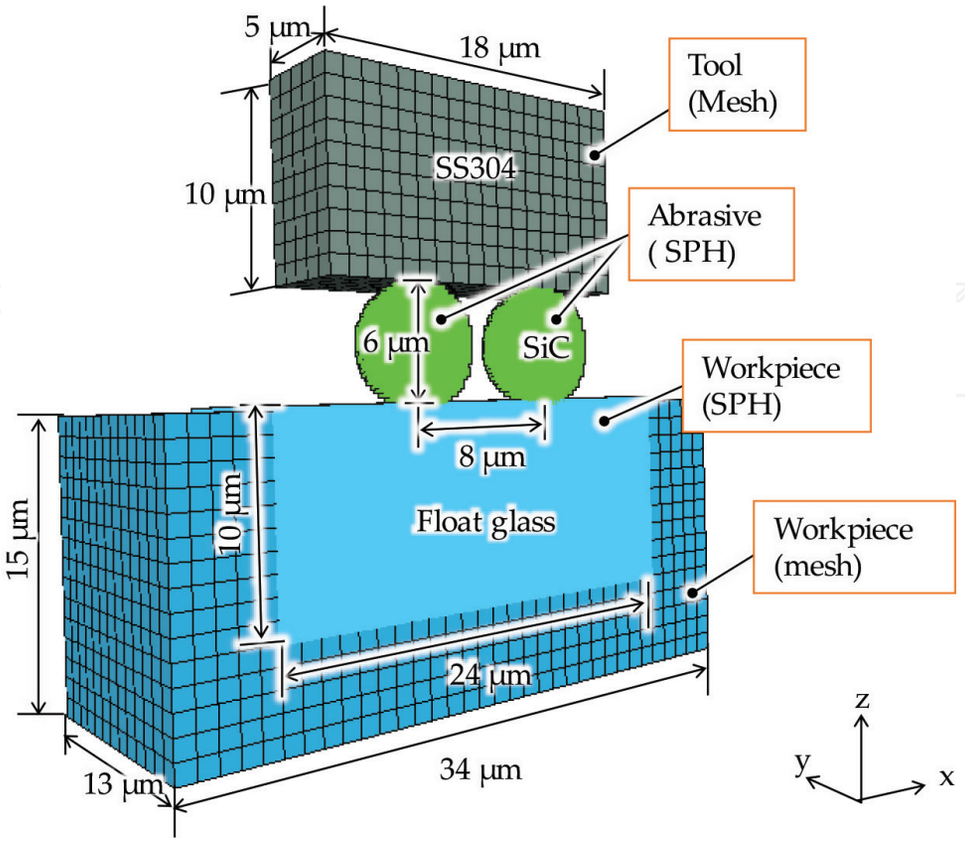

Figure 6. Snapshot of the initial state of the simulation model for two abrasive particles.

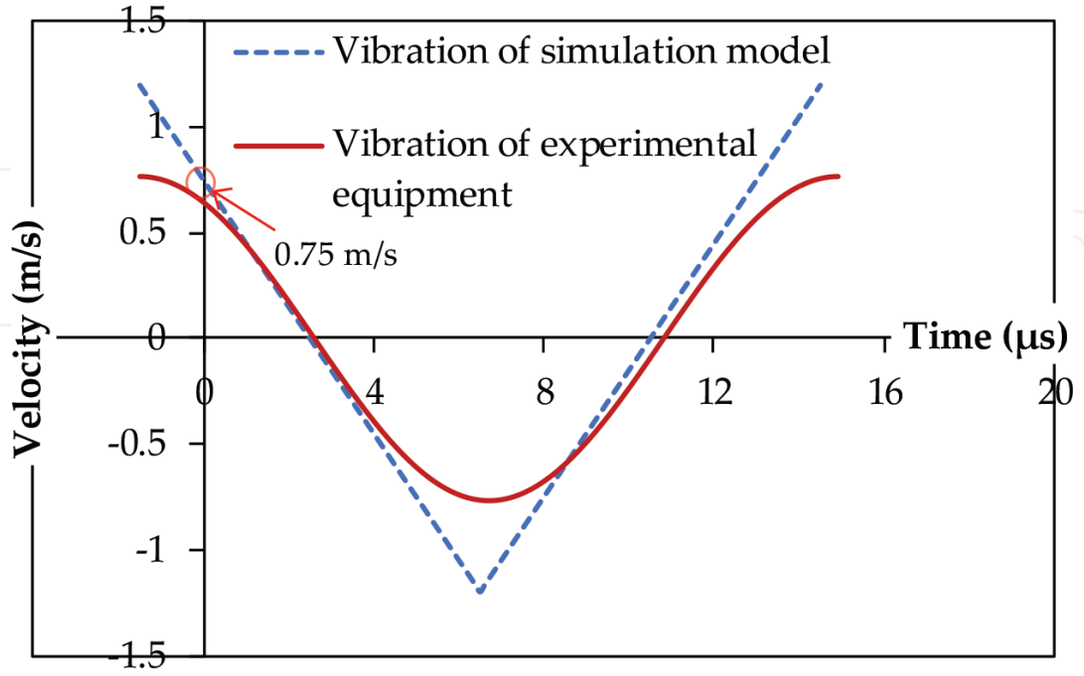

Figure 7. Velocity condition of the ultrasonically vibrated tool.

http://dx.doi.org/10.5772/intechopen.75170

condition is approximated to be linear variation in the simulation model. Even though the force between the tool and the abrasive particle may alter the tool motion, it is assumed that the velocity variation keeps linear in the whole calculation. The tool velocity condition was applied to nodes on the top surface of the tool, and the calculation starts with the velocity value of 0.75 m/s. All nodes on the bottom and side surfaces of the workpiece were constrained in the direction of z and x/y axes, respectively. Before calculation, the tool tip surface and the work surface are completely flat. As the tool starts to touch the abrasive and forces the abrasive to penetrate into the workpiece, all parts begin to deform or fracture. The contacts between the abrasive and the tool and the abrasive and the workpiece were assumed frictionless. Effect of the liquid in slurry and its flow on the material removal is negligible, which means that only the abrasive particle was considered.

3.1.4. Simulation results

The time-dependent simulation results along X-Z symmetric plane are shown in **Figure 8**. The colors shown in the figure represent the state of the material. The green, blue, and red

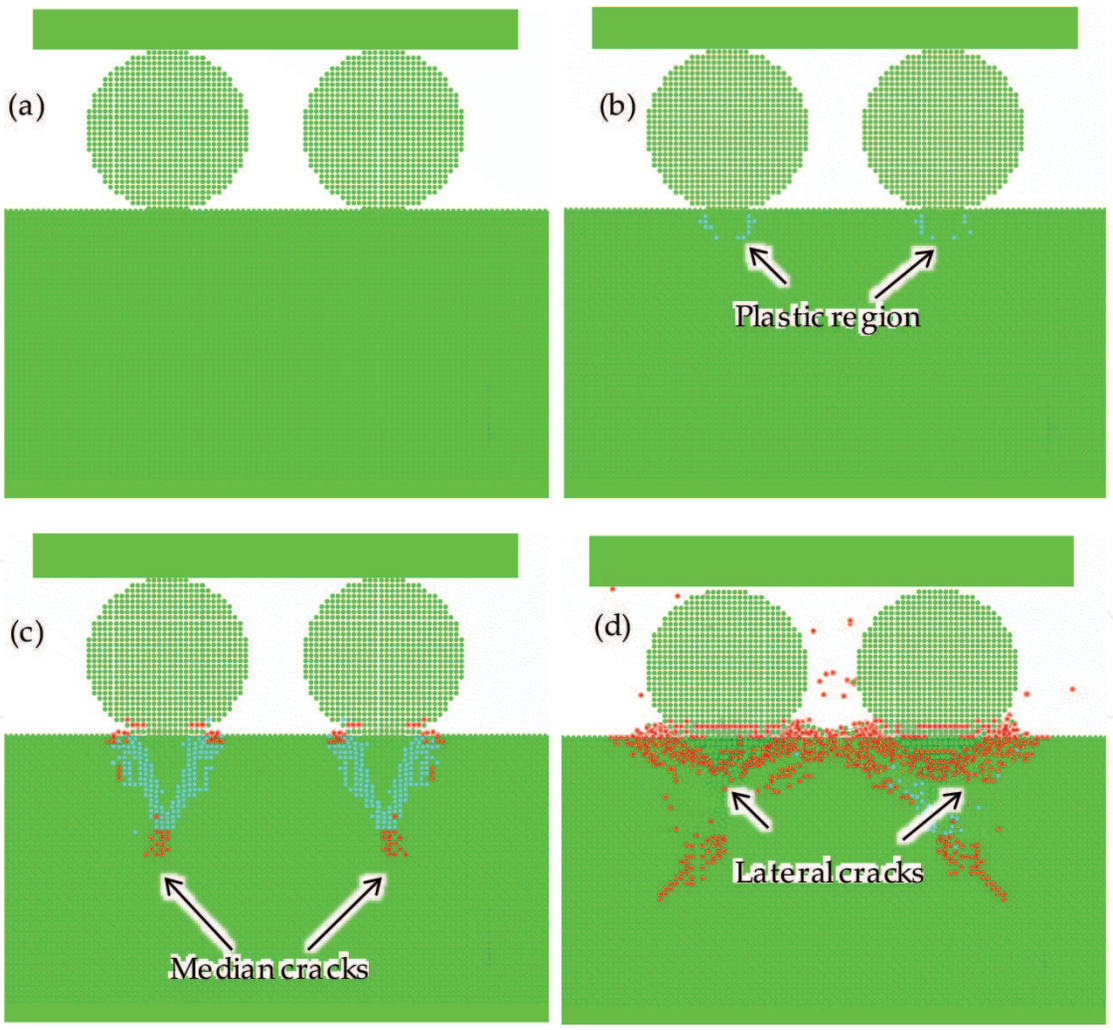

Figure 8. Simulation results of hammering actions by two adjacent abrasive particles: (a) initial condition, (b) after 0.1 μs, (c) after 0.25 μs, and (d) after unloading.

elements indicate elastic, plastic, and failure states, respectively. After 0.1 μs calculation, plastic zone induced by each of the two abrasive particles can be confirmed from the workpiece beneath the hammering location as shown in **Figure 8(b)**, which is the same as the result obtained from the single hammering calculation. With increase of the penetration of the tool, the median cracks initiate and propagate as shown in **Figure 8(c)**. A simultaneous fracture of the abrasives is also observed. With further penetration imposed by the tool, the cracks indicated in **Figure 8(c)** propagated into the surrounding material at an angle to the load axis instead of propagating parallel to the loading axis beneath the impact surface. In addition, the crushing of work material near the hammering site that is caused by each of the two abrasive particles became larger and larger as the loading displacement increases and finally coalesced. **Figure 8(d)** shows the final results after unloading. The lateral cracks also developed and propagated nearly parallel to the work surface after unloading.

3.1.5. Effect of the distance between impacts

Calculations were conducted by varying the distance between abrasive particles, and the results are shown in **Figure 9**. When the distance is within a specific range, the cracks are coalesced in the region between the impacts. With the increase of the distance between the two particles, the crack distribution becomes more similar to the one developed by a single impact, which means the interaction of the adjacent abrasive on the stresses in the region between two particles is decreased. The change of the material removal rate of the workpiece versus the distance between two adjacent abrasive particles is depicted in **Figure 10**. The material removal rate was defined as the mean volume of the materials removed by the mass of the two particles. It is noted that the interference between the two abrasive particles decreases when the distance between the two adjacent abrasive particles increases, which

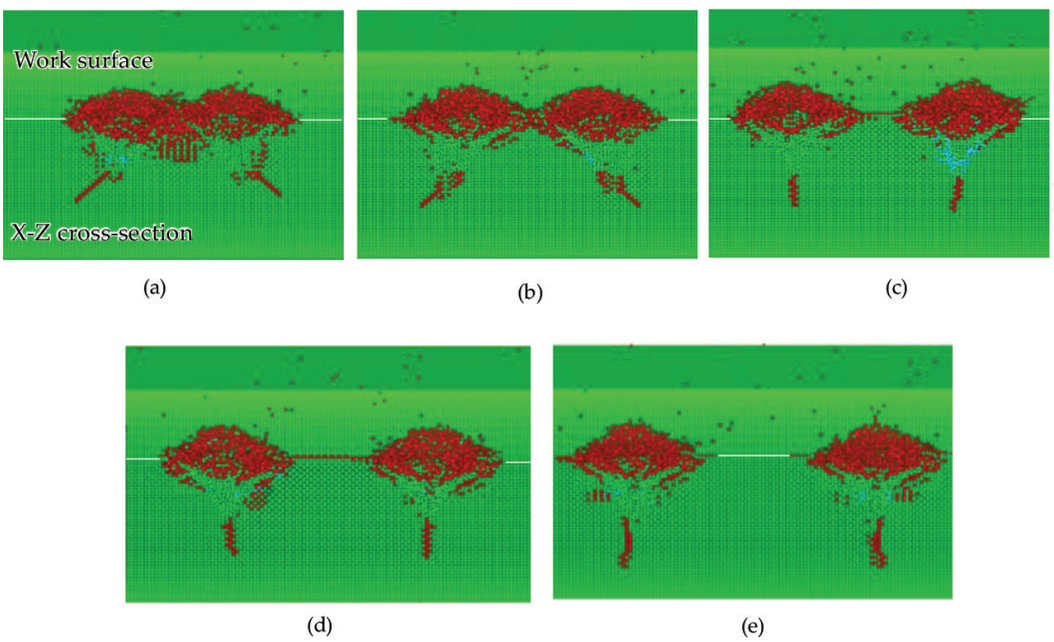

Figure 9. Effect of the distance between impacts: (a) 6.5 μm, (b) 8 μm, (c) 10 μm, (d) 12 μm, and (e) 14 μm.

http://dx.doi.org/10.5772/intechopen.75170

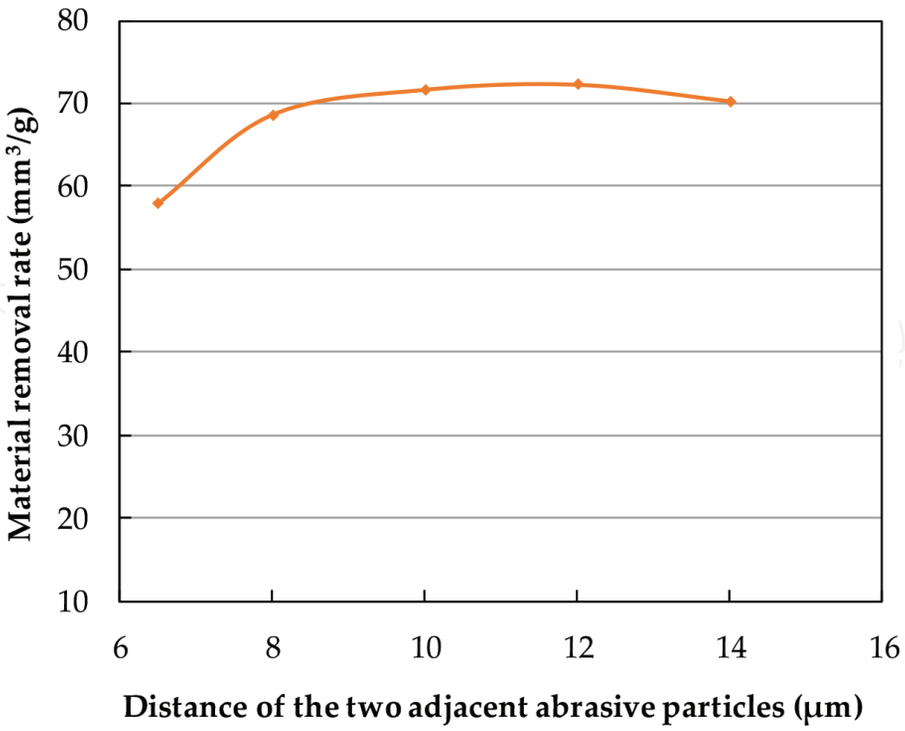

Figure 10. Effect of the distance between impacts on material removal of the workpiece.

increases the material removal rate. However, when a certain distance is exceeded, the interaction effect of the two adjacent abrasive particles is lost and the material removal would not be increased any more. The optimal distance for enhancing material removal rate was found to be 12 μm, twice the particle diameter.

3.2. USM experiments for verifying the simulation results

3.2.1. Experimental methods

USM experiments were conducted with different slurry concentrations for investigating the effect of the distance change among the abrasive particles. **Table 3** lists the experimental conditions. The machining was carried out with no circulation of slurry, and no tool feed was applied on the tool. A noncontact laser probe profilometer (Model: NH-3SP; Mitaka Kohki Co. Ltd., Japan) was used to scan across the machined area, and the volume of material removal was obtained by analyzing the three-dimensional surface topography. The cross sections of the machined surfaces were then created and examined using a scanning electron microscope (Model: SUI510; Hitachi Co. Ltd., Japan).

3.2.2. Experimental results

Figure 11 shows a schematic diagram of the experiment. In the simulation, only two particles were considered. However, there are a large number of abrasive particles worked on the workpiece in practical USM. Therefore, in order to verify the simulation results, the two parameters, i.e., material removal rate and distance of the two adjacent abrasive particles,

Vibration frequency (kHz)	61
Vibration amplitude (μm)	4 (peak to peak)
Tool material	SS304
Workpiece material	Glass
Abrasive (mesh size)	SiC #2000 (mean size, 8.4 μm)
Concentration of abrasive slurry	5, 10, 20, 30, 40, and 50 wt% mixed with water
Distance between workpiece and tool (μm)	10
Machining time (s)	30

Table 3. Experimental conditions.

were defined for comparison. The material removal rate was calculated as the volume of the materials removed from the workpiece divided by the mass of abrasive particles in the machining zone as shown in **Figure 11**. The distance between two adjacent abrasive particles in the slurry was calculated from the slurry concentration according to a formula taken from previous work [29]:

$$C = \frac{(\pi/6)\, d_0^3\, \eta \rho_g}{\lambda^2 d_0^3 \rho_g + (\pi/6)\, d_0^3\, \eta(\rho_g - \rho_e)} \times 100. \tag{1}$$

in which abrasive particles with the same diameter d_0 are supposed to be equally distributed in the machining area and schematically shown in **Figure 12**. λd_0 is the distance between the two adjacent abrasive particles, C is the slurry concentration, η is the volumetric efficiency of the abrasive particle, ρ_g is the density of the abrasive material, and ρ_e is the density of the slurry medium. In this work, the abrasive particle is SiC and the slurry medium is water; the corresponding densities are $\rho_g = 3.2$ g/cm^3 and $\rho_e = 1$ g/cm^3, respectively. Parameter $\eta = 90\%$, which

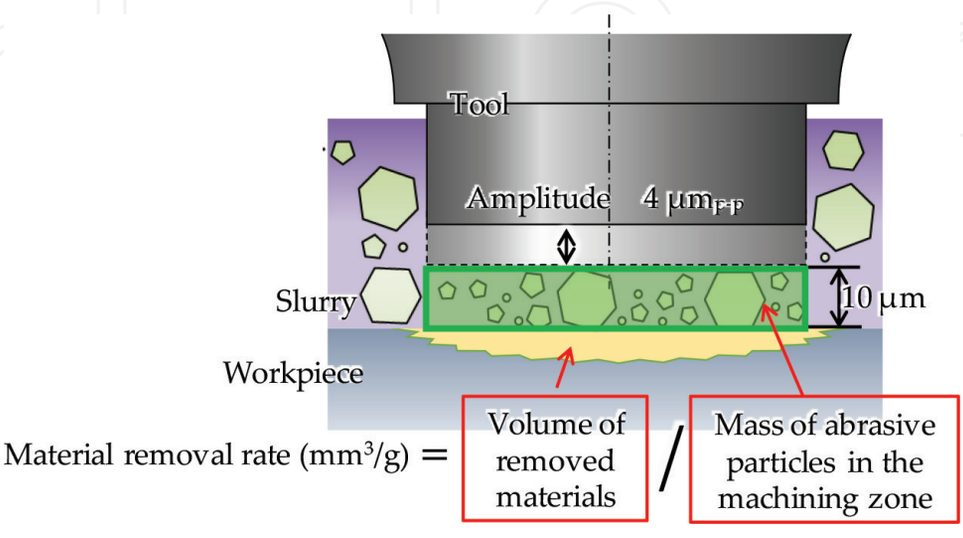

Figure 11. Schematic diagram of the experiment.

http://dx.doi.org/10.5772/intechopen.75170

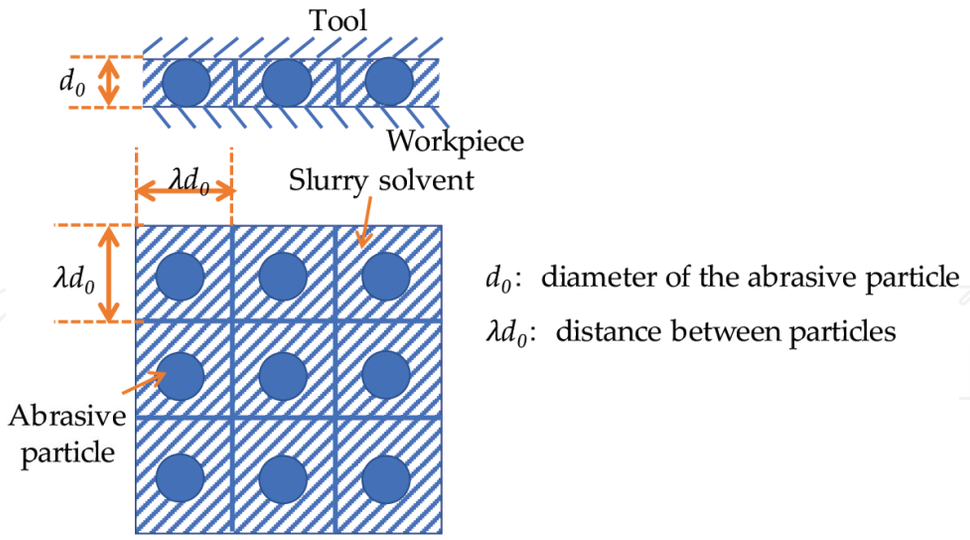

Figure 12. Distribution of abrasive particles in the machining area.

was determined by analyzing the abrasive particle shape using a particle analyzer (Model: Sysmex FPIA-3000; Malvern Instruments Ltd.). By substituting these values, λ under different slurry concentrations can be obtained. The relationship between the material removal rate and λ was determined and compared with the simulation results as shown in **Figure 13**. The simulation results were obtained from **Figure 10**, where the description of X axis was changed to λ by dividing the particle diameter 6 μm used in the model. The values obtained from

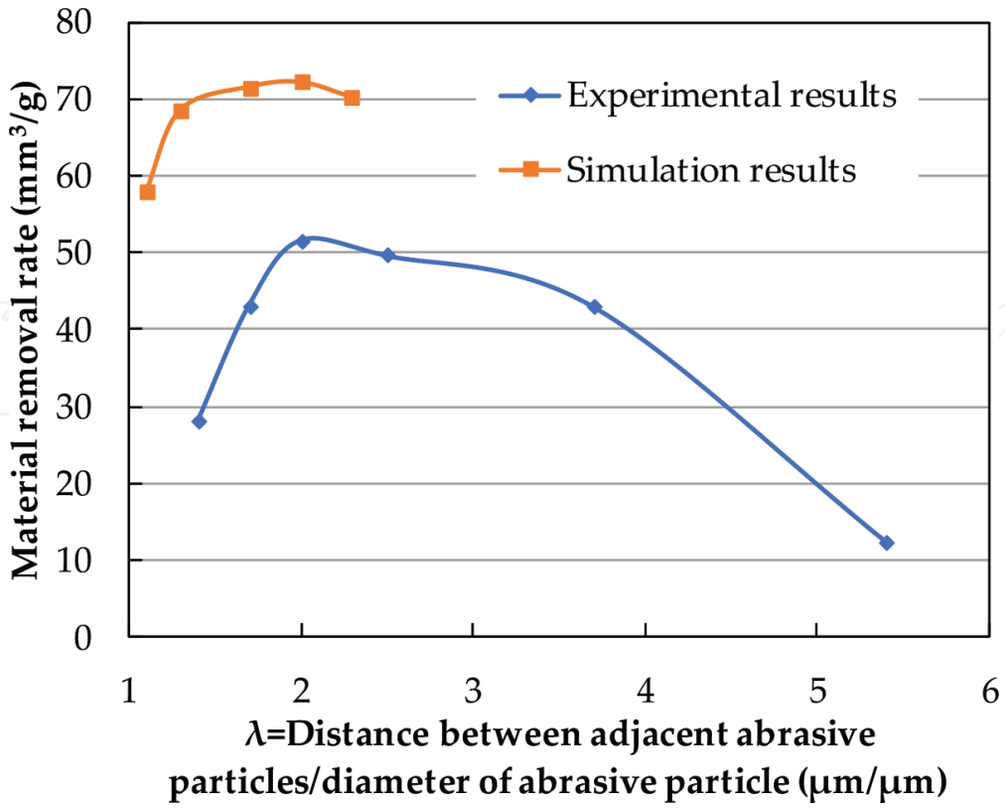

Figure 13. Effect of the distance between two adjacent abrasive particles on material removal rate.

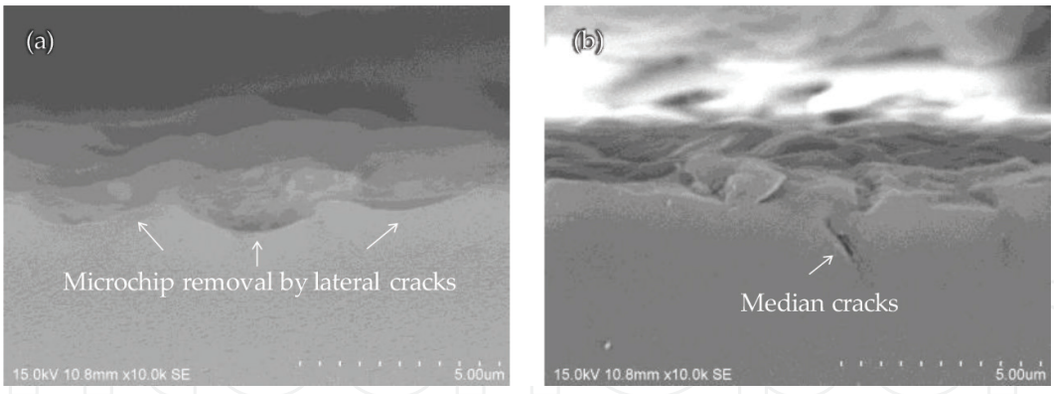

Figure 14. Cross sections of the machined surfaces: (a) microchip removal by lateral cracks, (b) example of median cracks.

the simulation results are constantly higher than those of experiments due to several factors including the nonuniformity of the abrasive particles in real machining process. However, both curves indicate that low material removal rate was obtained when the two adjacent abrasive particles are either very close or extremely far away. Maximum material removal was developed only when the distance between the impacting abrasive particles is optimal, which is found to be equal twice the diameter of abrasive particle from these results.

Although the material removal rate is influenced by slurry concentrations, the machined surfaces showed the same topography because materials are removed by the accumulation of cracks. **Figure 14** presents the SEM micrographs of cross sections of the surface machined by USM. From the micrographs, material removal via microchips which were occurred by the accumulation of lateral cracks can be confirmed. In **Figure 11(b)**, the median cracks remaining in the workpiece can also be observed. Both of the simulation and experimental results indicate that the material removal during USM is mainly caused by the accumulation of lateral cracks, while the median crack may play a less role. In addition, the median cracks that remain in the workpiece may cause subsurface defects and accordingly lower the quality of machined surface.

4. Summary and prospect

The current work introduced the background of the USM firstly. The importance of developing efficient micromachining technology for hard and brittle materials was stated. By comparing several machining processes, the potentiality of USM in micromachining of various hard and brittle materials was pointed out. Then, smoothed particle hydrodynamics method was proposed to study the material removal in USM and to reveal the influence of distance between two adjacent abrasive particles. The model was proven capable of simulating the crack generation in USM and helpful for predicting the machining results.

As the machining requirements of modern electronical, optical, and automotive components are getting stricter, there still exist many problems to be solved in the future for putting USM into practical industry. In micro-USM, the volume of material removed per stroke is very little due to the use of micrometer size abrasive particles. In fact, the corresponding machining speed is slowed down in order to obtain high form accuracy and superior surface finish

without large damages. However, with respect to a brittle material, microcracks are expected to be generated during this process and accordingly left on the machined surface. It is therefore important to find ways to remove these surface/subsurface cracks with no sacrifice of the machining speed, which means that the best balance machining conditions should be explored. A deep understanding of the mechanism and the effect of each machining parameter on USM needs to be given in future works.

Acknowledgements

The author gratefully acknowledges the support from Professor Tsunemoto Kuriyagawa, Associate Professor Masayoshi Mizutani, and Assistant Professor Keita Shimada at Tohoku University in Japan for their kind suggestions of my research work. The author would also like to thank Taga Electric Corporation in Japan with respect to the manufacture of USM tool and SmartDIYs Corporation for the provision of laser cutter parts for crack repair in the experiments.

The author would like to thank the financial support of "the Fundamental Research Funds for the Central Universities," China [Grant no. 3132018259].

Conflict of interest

The author(s) declared no potential conflicts of interest with respect to the research, authorship, and/or publication of this article.

Author details

Jingsi Wang

Address all correspondence to: jixiewangjingsi@hotmail.com

Marine Engineering College, Dalian Maritime University, Dalian, China

References

[1] Brow RK, Schmitt ML. A survey of energy and environmental applications of glass. Journal of the European Ceramic Society. 2009;**29**(7):1193-1201. DOI: 10.1016/j.jeurceramsoc.2008.08.011

[2] Tsuboi R, Kakinuma Y, Aoyama T, Ogawa H, Hamada S. Ultrasonic vibration and cavitation-aided micromachining of hard and brittle materials. Procedia CIRP. 2012;**1**:342-346. DOI: 10.1016/j.procir.2012.04.061

[3] Markov AI, Neppiras EA. Ultrasonic Machining of Intractable Materials. Iliffe: Scripta Technica, Inc.; 1966

[4] Klocke F, Dambon O, Capudi Filho GG. Influence of the polishing process on the near-surface zone of hardened and unhardened steel. Wear. 2005;**258**:1794-1803. DOI: 10.1016/j.wear.2004.12.015

[5] Komaraiah M, Reddy PN. A study on the influence of workpiece properties in ultrasonic machining. International Journal of Machine Tools and Manufacture. 1993;**33**(3):495-505. DOI: 10.1016/0890-6955(93)90055-Y

[6] Egashira K, Masuzawa T. Microultrasonic machining by the application of workpiece vibration. CIRP Annals – Manufacturing Technology. 1999;**48**(1):131-134. DOI: 10.1016/S0007-8506(07)63148-5

[7] Baek DK, Ko TJ, Yang SH. Enhancement of surface quality in ultrasonic machining of glass using a sacrificing coating. Journal of Materials Processing Technology. 2013;**213**(4):553-559. DOI: 10.1016/j.jmatprotec.2012.11.005

[8] Tateishi T, Yoshihara N, Kuriyagawa T. Fabrication of high-aspect ratio micro holes on hard brittle materials—Study on electrorheological fluid-assisted micro ultrasonic machining. In: The 4th International Conference on Leading Edge Manufacturing in 21th Century (LEM21); 2007

[9] Thoe TB, Aspinwall DK, Wise MLH. Review on ultrasonic machining. International Journal of Machine Tools and Manufacture. 1998;**38**(4):239-255. DOI: 10.1016/S0890-6955(97)00036-9

[10] Ghabrial SR. Trends towards improving surfaces produced by modern processes. Wear. 1986;**109**(1):113-118. DOI: 10.1016/0043-1648(86)90256-5

[11] Sun X, Masuzawa T, Fujino M. Micro ultrasonic machining and its applications in MEMS. Sensors and Actuators A: Physical. 1996;**57**:159-164. DOI: 10.1016/S0924-4247(97)80107-0

[12] Ichida Y, Sato R, Morimoto Y, Kobayashi K. Material removal mechanisms in non-contact ultrasonic abrasive machining. Wear. 2005;**258**(1):107-114. DOI: 10.1016/j.wear.2004.05.016

[13] Kumar J, Khamba JS. Modeling the material removal rate in ultrasonic machining of titanium using dimensional analysis. The International Journal of Advanced Manufacturing Technology. 2010;**48**:103-119. DOI: 10.1007/s00170-009-2287-1

[14] Zarepour H, Yeo SH. Predictive modeling of material removal modes in micro ultrasonic machining. International Journal of Machine Tools and Manufacture. 2012;**62**:13-23. DOI: 10.1016/j.ijmachtools.2012.06.005

[15] Singh R, Khamba JS. Taguchi technique for modeling material removal rate in ultrasonic machining of titanium. Materials Science and Engineering A. 2007;**460**:365-369. DOI: 10.1016/j.msea.2007.01.093

[16] Agarwal S. On the mechanism and mechanics of material removal in ultrasonic machining. International Journal of Machine Tools and Manufacture. 2015;**96**:1-14. DOI: 10.1016/j.ijmachtools.2015.05.006

[17] Kainth GS, Nandy A, Singh K. On the mechanics of material removal in ultrasonic machining. International Journal of Machine Tool Design and Research. 1979;**19**(1):33-41. DOI: 10.1016/0020-7357(79)90019-2

[18] Lee TC, Chan CW. Mechanism of the ultrasonic machining of ceramic composites. Journal of Materials Processing Technology. 1997;**71**(2):195-201. DOI: 10.1016/S0924-0136(97)00068-X

[19] Katahira T, Shimada K, Zhou T, Yan J, Kuriyagawa T. Material removal mechanism of ultrasonic machining. Journal of the Japan Society for Abrasive Technology. 2012;**56**(2):108-111. DOI: 10.11420/jsat.56.108

[20] Yu Z, Hu X, Rajurkar KP. Influence of debris accumulation on material removal and surface roughness in micro ultrasonic machining of silicon. CIRP Annals—Manufacturing Technology. 2006;**55**(1):201-204. DOI: 10.1016/S0007-8506(07)60398-9

[21] Guzzo PL, Shinohara AH, Raslan AA. A comparative study on ultrasonic machining of hard and brittle materials. Journal of the Brazilian Society of Mechanical Sciences and Engineering. 2004;**26**(1):56-61. DOI: 10.1590/S1678-58782004000100010

[22] Komaraiah M, Reddy PN. Relative performance of tool materials in ultrasonic machining. Wear. 1993;**161**:1-10. DOI: 10.1016/0043-1648(93)90446-S

[23] Hocheng H, Kuo KL, Lin JT. Machinability of zirconia ceramics in ultrasonic drilling. Materials and Manufacturing Processes. 1999;**14**(5):713-724. DOI: 10.1080/10426919908914864

[24] Johnson GR, Holmquist J. A computational constitutive model for brittle materials subjected to large strains, high strain rates and high pressures. In: Shock-Wave and High-Strain-Rate Phenomena in Materials. New York: Marcel Dekker; 1992. pp. 1075-1081

[25] Johnson GR, Holmquist TJ. An improved computational constitutive model for brittle materials. High-Pressure Science and Technology. 1994:981-984

[26] Holmquist TJ, Johnson GR, Grady DE, Lopatin CM, Hertel Jr ES. High strain rate properties and constitutive modeling of glass. In: Proceeding of the 15th International Symposium on Ballistics; 1995. p. 237

[27] Holmquist TJ, Johnson GR. Response of silicon carbide to high velocity impact. Journal of Applied Physics, Livermore. 2002;**91**(9):5858-5866. DOI: 10.1063/1.1468903

[28] Steinberg DJ. Equation of State and Strength Properties of Selected Materials. Livermore: Lawrence Livermore National Laboratories; 1996

[29] Sato K, Matsui M. Seimitsu Shiagehou (Precision Finishing). Kyoritsu Shuppan, Tokyo; 1958 (in Japanese)

IntechOpen